Flux measurements on ferromagnetic microprobes by electron holography

G. Matteucci and M. Muccini*
Department of Physics, University of Bologna, via Irnerio 46, 40126 Bologna, Italy

U. Hartmann
Experimental Physics Department, University of Saarbrücken, D-66041 Saarbrücken, Federal Republic of Germany and Institute of Thin Film and Ion Technology, KFA-Jülich, Federal Republic of Germany
(Received 19 April 1994)

Bulk ferromagnetic microprobes, as commonly used in magnetic force microscopy, have been analyzed by electron holography. Using the double exposure technique, detailed holograms have been obtained from nickel probes. The resulting two-dimensional interferograms can be well reproduced by numerical calculations which are based on the assumption that the probes stray field is produced by a macrodipole of several micrometers in length. By treating the dipole charge as a variational free parameter to be fitted against the experimental data, it is possible to determine the stray field produced by the probes, their effective leakage flux, and the surface area of a sample which may seriously be affected by the probes stray field. The results are considered especially important for those applications of magnetic force microscopy where the sample is likely to be magnetically perturbed by the stray field which is produced by the imaging probe itself.

I. INTRODUCTION

Magnetic force microscopy,[1] an offspring of atomic force microscopy,[2] permits the imaging of near-surface magnetic microfields at sub-100-nm lateral resolution.[3] A sharp ferromagnetic tip, attached to a flexible cantilever beam is employed in a standard force microscope setup to sense magnetostatic probe-sample interactions in the noncontact mode of operation.[4] The technique is of considerable importance for imaging the magnetic structure of media and devices used in the magnetic recording industry.[5] The major strength of magnetic force microscopy (MFM) in comparison to other high-resolution observation techniques, namely techniques based on electron microscopy, is that neither a special sample preparation nor vacuum conditions are required for operation. Concerning basic micromagnetic research, new possibilities arise from the fact that MFM is sensitive enough to image individual interdomain boundaries in a variety of hard and soft magnetic media.[6]

Many industrial and basic research applications of MFM suffer from uncertainties in image interpretation.[4] Sometimes even qualitatively different images from one sample are obtained if different microprobes are used.[7] Perturbations of the magnetic object under investigation, caused by the sensing tip itself, have clearly been observed.[8] The accurate qualitative and especially quantitative image characterization as well as the analysis of possible probe-induced artifacts relies on detailed knowledge of the inherent magnetic structure of the sharp ferromagnetic microprobes used for detecting sample stray fields. Both electrochemically etched polycrystalline ferromagnetic wires and nonmagnetic tips coated by thin ferromagnetic films are widely used as sensors in MFM. From a theoretical point of view, detailed calculation of the internal magnetic structure as well as of the stray magnetic field produced at the near-apex exterior of the sensors seems hopelessly complicated. This is on the one hand due to the morphologic and geometric boundary conditions which are in any case not known in detail. On the other hand, even if the geometry of a tip prepared by etching or thin-film deposition would be known in complete detail, the *ab initio* micromagnetic calculation would be extremely complicated since the magnetization vector field at a scale of that of interdomain boundaries is of interest.

The direct experimental observation of the magnetic structure of a sensor, which itself is used for one of the most highly resolving magnetic observation techniques, is by its very nature also a problem. A sufficient resolution would of course only be provided by electron microscopy based techniques. A considerable restriction to the application of these techniques is, however, provided by the problem that MFM sensors are usually not transparent to electron beams. This rules out immediately all transmission microscopy techniques. On the other hand, experimentally directly accessible is the magnetic stray field produced close to the apex of a sharp ferromagnetic tip. Using, e.g., Lorentz microscopy, the microfield configuration can be studied at least in an integral way by measuring the total deflection along the trajectories of electrons passing close to the ferromagnetic tip.[9]

In recent papers,[10,11] we have shown that electron holography is a promising alternative to study the fringe field produced by any kind of sharp ferromagnetic sensor. This technique which also involves integral averaging in one dimension, i.e., along the electron trajectories, directly provides high-resolution topological maps from which the spatial flux distribution in close vicinity to the probe's apex can be deduced. Combining the experimental data with suitable models for the magnetic charge arrangement within the tip then yields largely complete informa-

0163-1829/94/50(10)/6823(6)/$06.00

tion about the sensor's magnetic behavior.

In the present contribution, a detailed discussion of the holographic method applied to the measurement of stray flux produced by sharp ferromagnetic tips is given. Furthermore, the double exposure technique is shown to be a useful tool to obtain reliable information about the near-apex field configuration of the tips.[12] Holographic data obtained on bulk nickel probes are presented. Additionally, the possibilities of contrast reconstruction based on a microscopic dipole model for the probes are discussed. It is shown how the combination of experimental and theoretical data provides information about the effective magnetic moment of the probes as well as about the amount of magnetic flux penetrating a sample which is located at some distance from the probe's apex. The amount of flux is a particularly important quantity in MFM because it determines whether the magnetic structure of a sample is affected by the presence of the probe.

II. FIELD MODEL AND HOLOGRAPHIC RECORDING METHOD

To study the leakage field generated by a thin magnetic tip we consider a very simple model in which the tip's apex is approximated by a macroscopic magnetic dipole of length $L=20$ μm, as shown in Fig. 1. Such a dipole length seems, according to the existing experimental data[13,14] realistic for soft magnetic sensor tips. From knowledge of the associated magnetic scalar potential given by

$$V_m(x,y,z)=\frac{Q_m}{4\pi}\left\{\frac{1}{[x^2+y^2+z^2]^{1/2}}-\frac{1}{[(x+L)^2+y^2+z^2]^{1/2}}\right\}, \quad (1)$$

where Q_m and L are the magnetic charge and the dipole length, we can calculate the three-dimensional components of the external field.

A computer simulation of the field arising from such a dipole can be obtained by exploiting the holographic recording principle and introducing suitable boundary conditions.

Electron holograms can be recorded by using an electrostatic biprism as an interferometry device,[15] as sketched in Fig. 2. A coherent electron beam (EB) moving in a direction parallel to the z axis, illuminates the tip (T) under investigation. The biprism wire (W) and the tip are arranged in a mutually perpendicular position along the x and y axes, respectively. By applying a suitable voltage to the central wire (W) with respect to the two

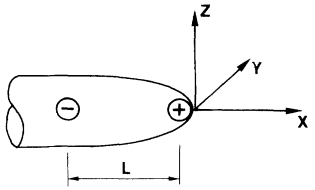

FIG. 1. Model for the magnetic tip apex.

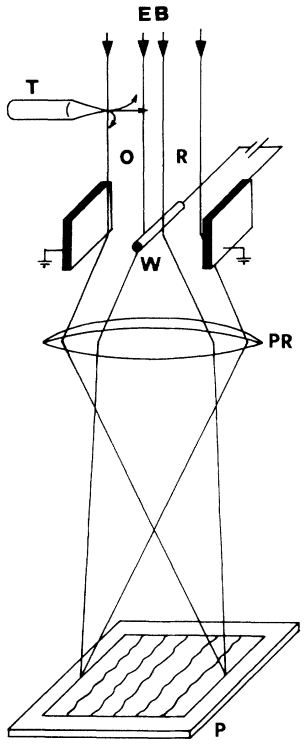

FIG. 2. Principle for hologram formation.

earthed plates, the part of the wave immediately adjacent to the tip apex (object wave O) is brought to interference, in the plane P, with part of the illuminating wave which travels a few microns distant (reference wave R). The latter is modulated by the leakage field of the tip. Therefore the phase difference between the object and reference waves will be recorded in the holograms.

According to the Aharonov-Bohm effect and using the Stokes theorem, the phase difference between the two interfering waves, revealed in the recording plane, can be written as

$$\Delta\varphi=\int_S\int \mathbf{B}\cdot\mathbf{n}\,dS\ , \quad (2)$$

where S is the total surface enclosed between the electron trajectories, $\mathbf{B}$ is the magnetic flux density, and $\mathbf{n}$ is a unit vector perpendicular to the surface. Therefore, with reference to Figs. 1 and 2, $\Delta\varphi$ is simply given by

$$\Delta\varphi(x,y)=\int_{-\infty}^{+\infty}dz\int_{x_1}^{x_2}B_y(x,y,z)dx\ , \quad (3)$$

where B_y is the y component of the magnetic flux density $\mathbf{B}$ generated by the linear dipole, x_1 and x_2 are the two points brought to interference. The result is that the holographic method allows the recording of two-dimensional maps arising as a projection of the investigated total field. Therefore, we look for a two-dimensional representation, in the symmetry plane x,y perpendicular to the beam direction z, of the leakage field around the vertex as a set of lines of force.

For this purpose, according to Eq. (3) and Fig. 2, we consider only the y component of the magnetic flux density in the plane x,y, i.e., $B_y(x,y,0)$. Since the phase

difference is related to the magnetic flux, the former can be calculated using Eq. (3), by performing the integral along z in an arbitrarily small neighborhood of the origin.

The result of this procedure is reported in Fig. 3, where an IBM PC/AT equipped with a video board able to display 512×512 pixels at 256 grey levels was used to simulate the lines of force around the tip apex T in the (x,y) plane. The field over all space can be figured out by allowing a complete revolution of the distribution of Fig. 3 around the x axis. The loci of points with constant phase are displayed as a set of curves with a phase difference of 2π between two successive black and white lines which enclose magnetic flux of h/e.

Having obtained a simulation of the dipole field in the x,y plane, let us consider what happens when the three-dimensional structure of the leakage field is taken into account. An ideal electron hologram will display the phase difference between the object wave, which travels along the z axis and is influenced by the whole leakage field, and a reference wave which is unperturbed (that is one which moves at an infinite distance from the apex). The phase difference recorded in such a hologram would be given by

$$\Delta\varphi(x,y)=\varphi(x=\infty,y)-\varphi(x=x_1,y)$$
$$=2y\frac{Q_m}{4\pi}\left\{-\frac{1}{y}\tan^{-1}\frac{x}{y}+\frac{1}{y}\tan^{-1}\frac{(x+L)}{y}\right\}_{x_1}^{\infty}. \quad (4)$$

The computer simulation of the contour map of the leakage field obtained by an ideal hologram is reported in Fig. 4. The dark lines are once more equiphase lines with a phase difference of 2π between successive lines; the number of lines in the map can be varied by changing the magnetic dipole charge. The striking difference of this map, in which the lines fan out radially from the tip apex T, with respect to that of Fig. 3, emphasizes the fact that, even from an ideal hologram, we cannot expect to display the field configuration directly.

Furthermore, in experiments we must consider that the reference beam, traveling at a distance of a few microns, is modulated by the leakage field of the tip. Therefore, the reconstructed hologram will show the loci of constant phase difference between the perturbed reference wave

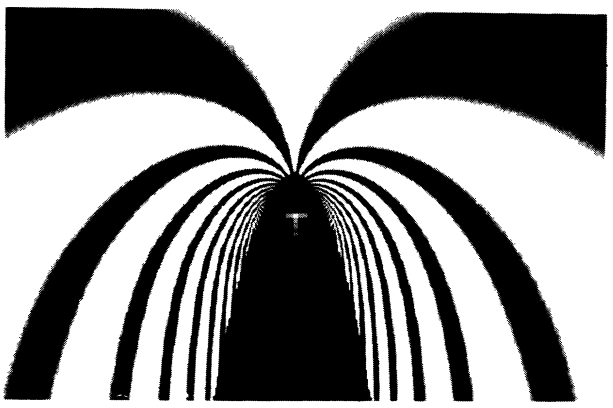

FIG. 3. Field arising from a magnetic macrodipole.

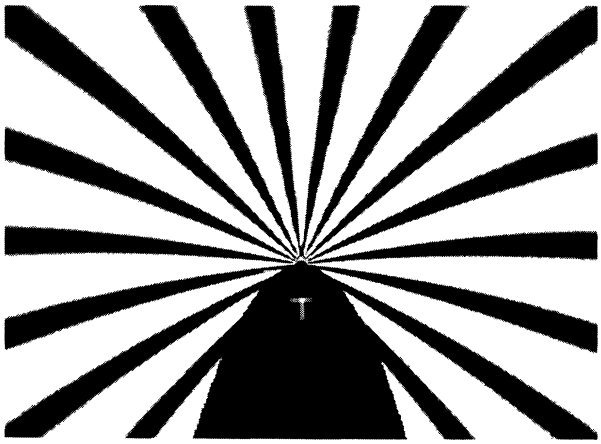

FIG. 4. Simulation of the leakage field contour map.

and the object wave. The phase difference $\Delta\varphi$ is given by

$$\Delta\varphi(x,y)=\varphi(x=x_2,y)-\varphi(x=x_1,y)\quad x_2-x_1=d\ , \quad (5)$$

where d is the distance between the points brought to interference. Figure 5 shows the simulated phase difference distribution according to Eq. (5). This is also the kind of map we expect by processing experimental holograms: the lines, starting from the tip apex T, assume a rounded shape and then join the tip itself. It is worthwhile to point out once more the striking difference between the expected maps for the leakage field, Fig. 5, and the actual trend of the field obtainable from Fig. 3.

III. EXPERIMENTAL METHODS

A. Preparation of MFM tips

Magnetic force microscopy is based on the spatially resolved detection of tiny magnetostatic interactions between a sharp ferromagnetic microprobe and a magnetic sample. Due to the long range of these magnetostatic interactions the mesoscopic geometry or, more precisely, the mesoscopic internal magnetic structure within a few

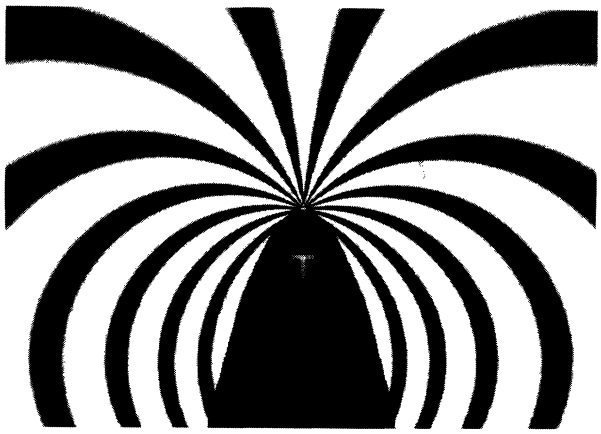

FIG. 5. Simulation of the phase difference arising when a perturbed reference wave is used.

hundred nanometers from the probe's apex, determines the imaging properties of the microscope. Thus, in contrast to many applications of the scanning tunneling microscope[16] or the contact-mode atomic force microscope,[2] the tip preparation technique plays a key role in successful imaging. For the nickel bulk tips used in the present analysis, the geometry-controlled shape anisotropy is the most important quantity for the ultimate imaging behavior of the probes.[4]

For the electrochemical preparation of the bulk ferromagnetic probes a polycrystalline nickel wire of an initial diameter between 100 μm and several hundreds of microns is exposed to the interface between two layered liquids. The lower one with the higher mass density is electrically insulating, while the upper one is the electrolyte. The nickel wire serves as one electrode while the counterelectrode is provided by a circumferential platinum wire. The latter is positioned in close proximity to the electrolyte-insulator liquid interface. Upon applying an ac voltage, the nickel wire is etched down to a diameter of a few microns within minutes. The ac voltage is then substituted by a dc voltage, changing the etching process to a polishing process. Periodic automatic tracing of the current-voltage curve underlying the electrolytic process determines the optimum current-voltage set point of the polishing procedure. This permits considerable smoothing of the wire's surface during the final reduction of its diameter. When the diameter reaches a certain critical value the wire's lower insulated part abruptly breaks due to the tensile stress caused by its own weight. This "dropoff method" performed at the sharp interface between the two liquids results in particularly sharp tips especially exhibited by the removed part of the wire. Fairly reproducible results were obtained by using $CHBr_3$ as the insulating liquid of high mass density. As electrolytes both 75% H_3PO_4 saturated with CrO_3 as well as a mixture of 33% H_2SO_4, 42% H_3PO_4, 2% HCl, 22% H_2O, and 1 wt. % $NiSO_4$ were used. After electrochemical preparation, the tips were tempered for a few hours in high vacuum to remove surface contamination and mechanical stress. Further details of the experimental methods were published elsewhere.[17]

B. Holographic recording

Electron holography is a well-known technique with which to study the object wave in both its amplitude and phase components.[18–21] In this way, a storage of the characteristic of the object in terms of the wave function in the recording plane is achieved. Once the object information has been transferred to the recording-plane level, it becomes of crucial importance to recover the actual amplitude and phase of the object wave function. This is nowadays a well established procedure if the reference wave used to record the hologram is not perturbed by interaction with the object. It is, however, not so straightforward if the reference wave is affected.[22] It has been demonstrated, from this point of view, that the most reliable method to be used is the double-exposure technique, which prevents the introduction of further possible uncertainties related to optical processing.

Off-axis image electron holograms were recorded by means of a Philips EM 400T electron microscope equipped with a field emission source and an electron biprism inserted at the selected area aperture level. The microscope is operated in the diffraction mode with the objective lens switched off, so as not to perturb the leakage field of the tip. The diffraction lens was used to focus the tip apex on the photographic plate and provided, together with the remaining lenses, an ultimate magnification of about 2000× at the final viewing screen.

In order to record reliable phase-difference maps of the leakage field of tiny magnetic tips, we used the double-exposure technique which allows display of the phase-difference information directly on the photographic plate. With the availability of an electron microscope equipped with a slow-scan CCD camera, the decodification of the field information would have been greatly simplified.

IV. INTERPRETATION OF THE EXPERIMENTAL RESULTS

A. Stray field analysis

In this section we discuss how to interpret experimental double exposure holograms taking advantage of simulations based on the dipole model for the tip apex.

Figure 6 reports a double exposure hologram in which the reference wave was perturbed. The interference field width is 4 μm. The region displayed above the apex T of the tip is crossed by black and white fringes which represent the loci of equal phase difference between the two exposures. The phase difference between two neighboring black (or white) fringes is 2π. The lines on the left part show different curvature with respect to those on the right side. This is due to the presence of the magnetic tip that, in order to perform the second exposure, was moved along its axis towards the bottom of the picture, and shifted slightly to the left side. If the tip were shifted further away, because of the strong leakage field, the second fringe system would have moved laterally to such an amount that superposition of the two holograms would be impossible.

The phase-difference lines do not directly display the magnetic stray field around the apex. In order to get the actual field trend we must first show that, starting from the field model, we can simulate the experimental phase distribution of Fig. 6. The resulting pattern is shown in Fig. 7; as it can be seen, the trend of the equiphase lines is in good agreement with the experimental results. Therefore the leakage field of the tip can be inferred, with good confidence, as that produced by a magnetic macrodipole.

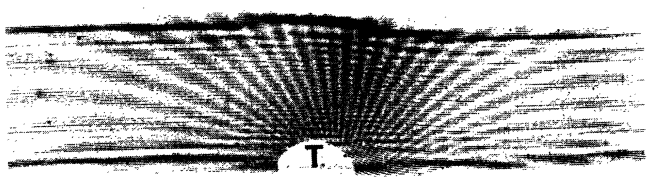

FIG. 6. Experimental double exposure hologram displaying the phase-difference map.

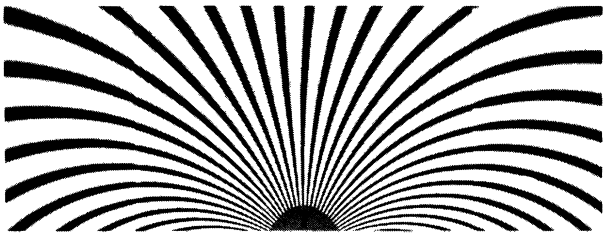

FIG. 7. Computer simulation of Fig. 6.

B. Measurement of the total leakage flux

Once the probe's magnetic behavior can be described within the framework of a macroscopic dipole model it is possible to determine those magnetic field quantities which are most relevant for the interaction of the probe with a potential sample in a real MFM application. From detailed comparison of the experimental and simulated holograms one can determine the dipole moment and its location with respect to the probe's apex. Since the dipole length is usually very large compared with those working distances which are relevant for MFM operation the discussion can be conveniently restricted to the near-field regime. In this regime only the near-apex charge of the dipole is relevant for the magnetostatic probe-sample coupling, i.e., the probe behaves like a magnetic monopole. The actual amount of charge and its location with respect to the probe's apex is known from fitting the simulated hologram to the experimental one. The probe's stray field can then be calculated at any plane located a certain distance from the probe's apex. Thus the magnetostatic interaction with a given sample can be analyzed.

It is instructive to get an idea about the total amount of leakage flux that would penetrate a fictitious sample imaged by the probe shown in Fig. 6. The simulated hologram of this probe is shown in Fig. 8. The horizontal line (1) close to the apex (T) indicates the surface of a sample at a working distance of 100 nm which may be considered as typical in MFM. The total flux penetrating the sample can now simply be determined by counting the number of successive black and white lines which involve a magnetic flux difference of h/e, respectively. One thus finds for the total flux penetrating the sample an amount of about $10h/e$. If, however, the working distance would be increased to about 2 μm, as indicated by line (2), the magnetic flux reaching the sample would be reduced to $1h/e$. The effective lateral range of probe-sample interaction, given by the length of the line (1) amounts to about 1 μm, and is the same as for the larger working distance indicated by line (2). The particularly low flux rates found in this example result from the low effective dipole charge which in turn reflects the dull probe geometry in Fig. 6.

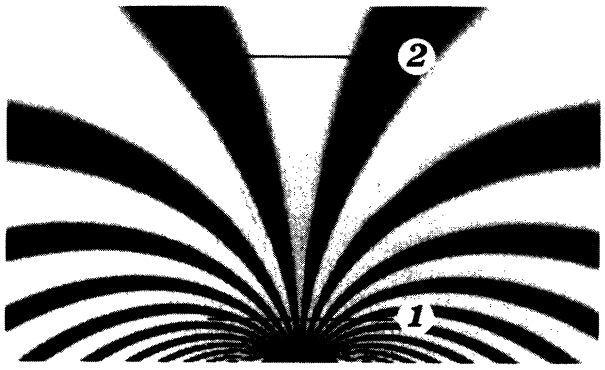

FIG. 8. Evaluation of the magnetic flux leaking from the nickel tip apex.

An accurate determination of the absolute amount of leakage flux and stray field in the sample plane is only possible if the probe can be modeled by a simple magnetic charge arrangement. However, even if the experimental hologram is much more complicated than that shown in Fig. 6, it is still possible to estimate the amount of flux at the sample surface. Again only the interference fringes involving a flux difference of h/e have to be counted. The problem often preventing a rigorously accurate flux determination consists of the fact that usually the exact location of the sample plane with respect to the probe apex cannot be determined. The reason is that the probe shadow in the experimental hologram can only be identified with some uncertainties (see Fig. 6). On the other hand, an estimate of the leakage flux with an uncertainty of a few h/e is often possible. The stray field could in this case, however, not be reconstructed since the detailed magnetic charge distribution producing the leakage flux cannot unequivocally be determined.

For the general situation of holographic imaging of magnetic microprobes we see three major limitations for accurate flux measurements: (1) For strongly inhomogeneous stray fields the interference fringes may become very tiny and the accuracy of the measurement is ultimately limited by the spatial resolution of the holographic imaging system. (2) Strongly inhomogeneous fields do, apart from causing wanted phase differences between image and reference electron waves, also exert unwanted Lorentz forces on the electron beams. Deflections result in shadows and perturbations in the holographic image. (3) Stray fields of sufficient range seriously affect the reference electron wave. This is accounted for in the present work by using a perturbed reference wave for numerical reconstruction of the holograms. This method is of course only possible if one knows how the reference wave is influenced by the stray field. This definitely requires knowledge of the magnetic charge distribution in the microprobe which produces the stray field. If this charge distribution is not known in detail, the stray-field-induced deformation of the reference wave cannot be figured out directly. The experimental data then only provide information about local flux differences in the exterior of the probe rather than about absolute flux rates.

V. DISCUSSION AND CONCLUSIONS

We have demonstrated that electron holography is a powerful technique for analyzing magnetic properties of MFM probes. The double exposure technique enables one to get detailed holograms which are particularly suitable for quantitative interpretation. By comparing the

experimental data with results from numerical simulations it was found that the stray field produced by nickel probes is largely equivalent to that produced by a macroscopic dipole of several micrometers length. Since, however, the dipole length is always large compared with those distances to the probe apex which are of interest for MFM applications, the adequate description of the probe's magnetic behavior can be based on a single magnetic charge of a certain amount located a given distance from the apex. The actual charge and distance values depend on the detailed spheroidal geometry, i.e., mainly on the radius of curvature of the probe.

Once the magnitude of the magnetic charge and its location with respect to the probe apex have been determined by comparing the experimental hologram with the simulated one, it is straightforward to determine the amount of leakage flux and stray field which interact with the sample if the respective probe is operated in a MFM. Furthermore, it is possible to estimate the effective range of the magnetostatic interaction between probe and sample which ultimately determines the achieved spatial resolution. It should, however, be emphasized that the holograms are taken from magnetic probes in free space. As soon as the probe is used in real MFM applications in close proximity to the sample, both probe and sample will usually respond in a nonlinear way. The interaction then results in a mutual deformation of probe and sample magnetization-vector fields. We thus consider the present results especially important for those MFM applications, where the probe-sample magnetostatic coupling is sufficiently weak. This is, e.g., the case if the sample is a dia- or paramagnet or a superconductor. In particular the investigation of superconductors by MFM is presently discussed as a very promising application.

Another important, more general, aspect is that the present investigations certainly help to better understand the detailed internal magnetic domain structure of MFM probes. In particular, the balance between shape anisotropy and magnetostatic energy contributions on the one hand, and magnetocrystalline and spin-exchange coupling contributions on the other hand has to be investigated in more detail in order to fabricate improved MFM probes. We think that, due to the performed holographic investigations, soft magnetic probes made out of iron or nickel are now relatively well understood with respect to their near-apex micromagnetic behavior. As expected, these probes usually show an extended single-domain configuration close to the apex. The domain length of typically a few micrometers make them behave as macroscopic dipoles in the far-field regime and as magnetic monopoles in the near-field regime which is relevant for MFM applications. Our future work in the field of holographic imaging will be concentrated on the investigation of hard magnetic bulk probes, e.g., made out of cobalt, and of thin-film probes made out of a variety of soft and hard magnetic materials. Very preliminary experimental results show that these probe types have much more complex behavior than the soft magnetic bulk probes. In any case, a complicated multidomain configuration will have to be taken into account rather than one single extended apex domain.

ACKNOWLEDGMENTS

This work was financially supported by MURST coordinated by Consorzio INFM and CNR-GNSM. We wish to gratefully acknowledge the skillful technical assistance of S. Patuelli.

---

*Present address: Institute of Molecular Spectroscopy-CNR, Via Gobetti 101, 40129 Bologna, Italy.

[1]Y. Martin and H. K. Wickramasinghe, Appl. Phys. Lett. **50**, 1455 (1987).

[2]G. Binnig, C. F. Quate, and C. Gerber, Phys. Rev. Lett. **56**, 930 (1986).

[3]U. Hartmann, J. Magn. Magn. Mater. **101**, 263 (1991).

[4]U. Hartmann, Adv. Electron. Electron Phys. **87**, 49 (1994).

[5]U. Hartmann, J. Vac. Sci. Technol. A **8**, 411 (1990).

[6]P. Gruetter, H. J. Mamin, and D. Rugar, in *Scanning Tunneling Microscopy II,* edited by R. Wiesendanger and H. J. Guentherodt, Springer Series in Surface Sciences, Vol. 28 (Springer-Verlag, Berlin, 1992), p. 151.

[7]T. Göddenhenrich, U. Hartmann, M. Anders, and C. Heiden, J. Microsc. **152**, 527 (1988).

[8]T. Göeddenhenrich, U. Hartmann, and C. Heiden, Ultramicroscopy **42-44**, 256 (1992).

[9]S. McVitie and U. Hartmann, in *Proceedings of the 49th Annual Meeting of the Electron Microscopy Society of America,* edited by J. N. Chapman (San Francisco Press, San Francisco, 1991), p. 92.

[10]G. Matteucci and M. Muccini, *Electron Microscopy,* Proceedings of the 10th European Congress on Electron Microscopy, edited by A. Ríos, J. M. Arias, L. Megías-Megías, and López-Galindo (Secretariado de Publicaciones de la Universidad de Granada, Granada, Spain, 1992), Vol. 1, p. 657.

[11]G. Matteucci, M. Muccini, and U. Hartmann, Appl. Phys. Lett. **62**, 1839 (1993).

[12]G. Matteucci, G. F. Missirolli, J. W. Chen, and G. Pozzi, Appl. Phys. Lett. **52**, 176 (1988).

[13]D. Rugar, H. J. Mamin, P. Guethner, S. E. Lambert, J. E. Stern, I. McFadyen, and T. Yogi, J. Appl. Phys. **68**, 1169 (1990).

[14]C. Schönenberger and S. F. Alvarado, Z. Phys. B **80**, 373 (1990).

[15]G. Möllenstedt and H. Düker, Z. Phys. **145**, 377 (1956).

[16]G. Binnig, H. Rohrer, C. Gerber, and E. Weibel, Phys. Rev. Lett. **49**, 57 (1982).

[17]H. Lemke, T. Göddenhenrich, H. P. Bochem, U. Hartmann, and C. Heiden, Rev. Sci. Instrum. **61**, 2538 (1990).

[18]A. Tonomura, Rev. Mod. Phys. **59**, 639 (1987).

[19]S. Frabboni, G. Matteucci, G. Pozzi, and M. Vanzi, Phys. Rev. Lett. **55**, 2196 (1985).

[20]G. Matteucci, G. F. Missiroli, E. Nichelatti, A. Migliori, M. Vanzi, and G. Pozzi, J. Appl. Phys. **69**, 1835 (1991).

[21]H. Lichte, in *Advances in Optical and Electron Microscopy,* edited by T. Mulvey (Springer, Berlin, 1991), Vol. 12, p. 25.

[22]G. Matteucci and M. Muccini, Ultramicroscopy **53**, 19 (1994).

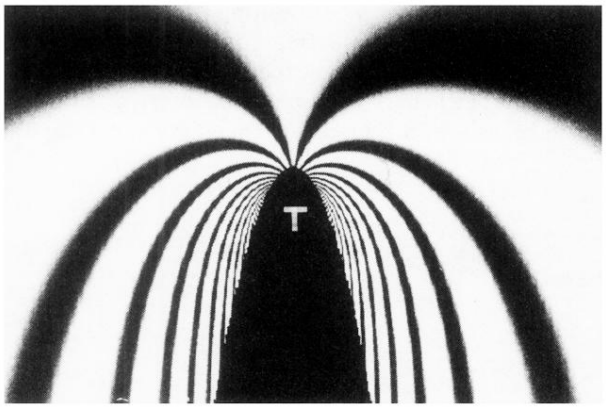

FIG. 3. Field arising from a magnetic macrodipole.

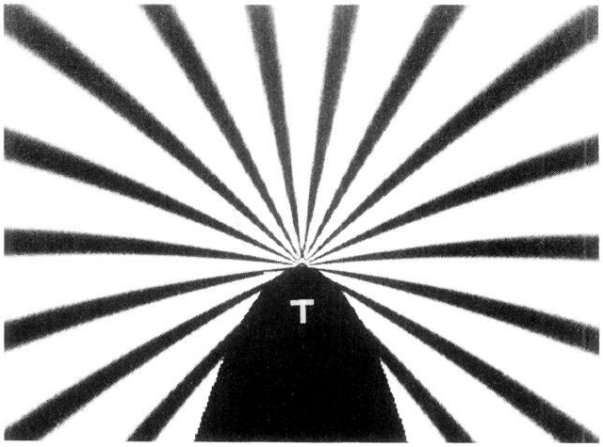

FIG. 4. Simulation of the leakage field contour map.

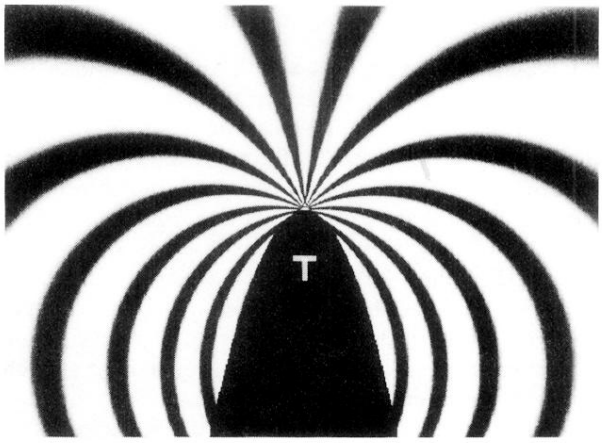

FIG. 5. Simulation of the phase difference arising when a perturbed reference wave is used.

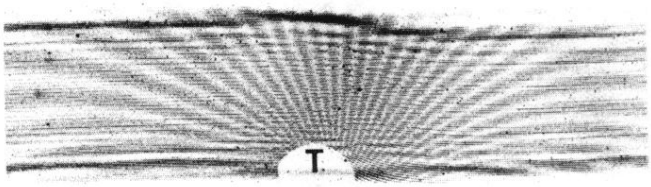

FIG. 6. Experimental double exposure hologram displaying the phase-difference map.

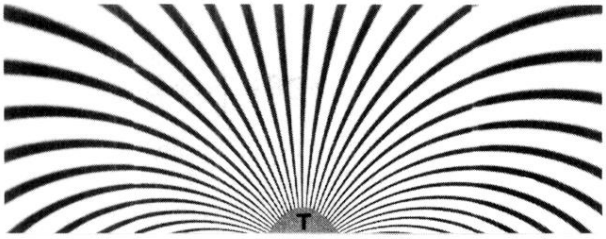

FIG. 7. Computer simulation of Fig. 6.

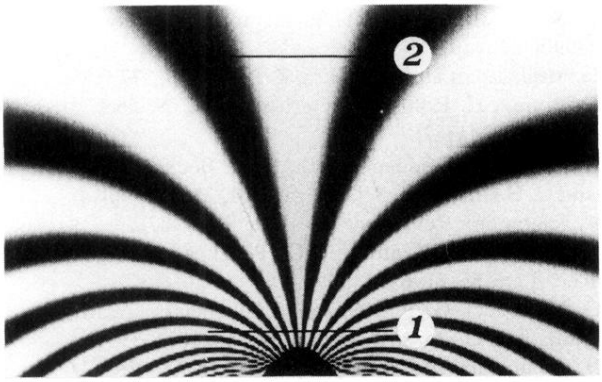

FIG. 8. Evaluation of the magnetic flux leaking from the nickel tip apex.